Communication

Energetics of $C_8B_8N_8$, $N_{12}B_{12}$, and C_{24} Macrocycles and Two [4]Catenanes

Lorentz Jäntschi [1,2]

1   Department of Physics and Chemistry, Technical University of Cluj-Napoca, 400641 Cluj-Napoca, Romania; lorentz.jantschi@gmail.com; Tel.: +40-264-40-1775
2   Chemical Doctoral School, Babes-Bolyai University, 400028 Cluj-Napoca, Romania

Abstract: Polyynes are alternations of single and triple bonds between carbon atoms, while cumulenes are successions of double bonds. Since the triple bond is the strongest bond between two carbon atoms, recent preoccupations included synthesizing and condensing cyclic polyynes and cumulenes and their clusters. Density functional theory calculations predicted stable monocyclic rings formation for a number of C atoms equal to or higher than 16. Alternative to the series of Carbon atoms are alternations of Boron and Nitrogen. Large rings (such as those of 24 atoms) can be crossed and thus small clusters can be formed. Patterns of three crosses seem to further stabilize the atomic ensemble. Clusters of $4C_{24}$ and $4B_{12}N_{12}$ (96 atoms) as well as $4C_{26}$ (104 atoms) have been designed, and their conformation has been studied here.

Keywords: polyyne; cumulene; catenanes; carbon rings; clusters; congeners

1. Introduction

It has been demonstrated that polyynes possess both metallic and semiconducting properties [1], being susceptible for valuable superconductivity [2], while a recent study [3] places its optical gap to below 1.6 eV. Properties of interest include tensile and chemical bond stiffness [4], the difference between lengths of single and triple bonds [5], resonant tunnel effect [6], and adjustable bandgap [7].

The recent rediscovery of polyyne molecules [8] is due to their unique features of single and triple bonds alternation. If a single C–C bond has an average distance of 1.53–1.54 Å and dissociation energy of 3.6–3.9 eV, then the presence of a double or of a triple bond updates these values to about 1.33 Å and 7.4 eV and to about 1.20 Å and 10 eV, respectively [9]. With an average decrease in distance of 22% relative to a single bond and of 13% relative to an aromatic bond, and an average increase in energy of 167% relative to a single bond and of 83% relative to an aromatic bond, this makes the triple bond between Carbon atoms very attractive for applications requiring dense materials [10] with very good compressibility [11]. Generally speaking, despite certain initial doubts [12], polyynes are the oligomeric cousins of carbene, being of scientific interest either as linear or cyclic complexes [13].

A polyyne-type $((-C\equiv)_n)$ structure is favoured over a cumulene-type $((=C=)_n)$ structure [14,15]. Valuable theoretical [15–18], experimental [19–22] and review [23–25] studies were conducted to characterize this polymer. A chain with $n > 300$ was firstly reportedly synthesized in 1995 [26], while an abundance of shorter chains ($n \leq 32$) was reported much earlier [27]. Very good results were obtained in [28] for medium sized chains (72%, 36%, and 51% for $n = 20$, 24 and 28, respectively). In addition, of interest and under investigation is trapping of linear polyynes in nanotubes [29].

Cyclic polyynes ($n = 10, 14$ and 18 in [30]; 24 in [31]) may provide further insight about stabilization of the polyynes. Moreover, old [32,33] and new [25,31] studies came to support the fact that certain rings are more stable than linear chains. Specifically, in [31], it is noted that rings are more likely to appear when $n \geq 14$ and $n = 4 \cdot k$ ($n = 16, 20, 24, 28, \ldots$).

The tendency of the polyynes to form rings was observed at laser vaporization of graphite as secondary product in the synthesis of fullerenes in [34] (when $22 \leq n \leq 46$). Pieces of evidence that crosslinking of the chains stabilizes molecules as a cluster are [35–37].

Replacement of Carbon atoms with Boron and Nitrogen may produce significant changes to the molecular properties; for a full factorial study, consult [38].

Information regarding the stability of polyyne rings is essential in the identification of new materials with valuable properties. In this communication, a series of previous findings regarding the stabilization of polyyne rings is revised, along with some new findings regarding the replacement of Carbon atoms with alternating Boron and Nitrogen (called here {B,N}-congeners).

The study is motivated by the possibility to obtain more complex molecular architectures starting from polyynes [18,39–41].

2. Background and Supporting Data

Cyclic polyynes and cumulenes are of peculiar interest since their dimensionality is expanded from 1D to 2D, and they possess a very good symmetry (in convergence to $C_{n/2}$).

Before proceeding, it should be pointed out that the terminology 'in convergence' is used here to reflect a state of facts: for small n, the stress over the strain due to bending of the molecule is high (bending angle is $2\pi/n$). Due to this stress, the atoms have the tendency to jump up and down relative to a plane of a virtually perfect circular molecule (jumps can alternate regularly or not); hypothetically, each of these configurations defines a conformation, but since the differences are very small (so small that the molecular modeling programs detect breaking of the symmetry order from time to time), those configurations will not be considered conformations and C_n polyyne molecule will be considered planar.

Crosses of polyynes and cumulenes can be the pillars of 3D architectures. According to [42], a more appropriate term would be [n]catenanes, where n is the number of macrocycles.

While molecular modeling may provide insights of the conformations and equilibriums at the atomic and molecular levels, regression analysis may cause an oversight of the whole process of formation and stabilization.

At first glance (see Figure 1), the association between Energy (E) and number of atoms (n) seems perfectly linear, with no other information to discover. Figure 1 was made using HF/STO-3G model data. One can observe almost a perfect association. Nevertheless, the intercept has no physical meaning despite of the fact that is statistically significant (Student's $t = 13.8$; probability to be 0: $p_t = 1.5 \times 10^{-9}$). However, this is due to the fact that the small variations (providing essential information about the molecular stability) are buried beneath big variations—adding a pair of atoms to the molecule adds a large amount of energy, much larger than the variation due to the increase or decrease in its stability.

$$\hat{E} = -37.9185n + 0.333732, \quad r^2 = 1.000000$$
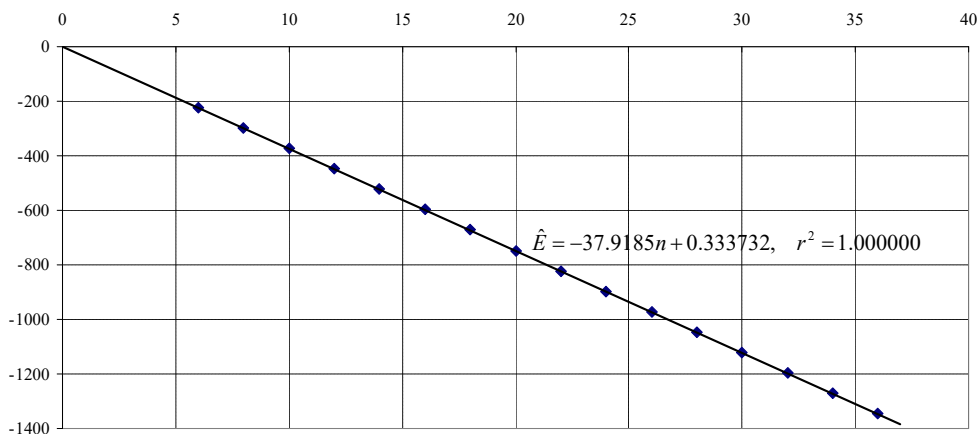
Figure 1. Energy (in a.u.) of C_n polyyne as function of n.

Some representative models were selected (see relative residual error in $\Sigma_{1 \leq i \leq 4} \Delta_{r,i}$ column in Table 1, models for $N \equiv N$ molecule, for the magnitude of estimation error).

Table 1. Experimental vs. calculated (at different theory levels) values for energy and distance between atoms at $N \equiv N$ molecule.

Method	S°	CV	ZPE	d	$\sum_{1 \leq i \leq 4} \Delta_{r,i}$
HF 0(10)	191.99	20.79	15.97	113.4	18.23
HF 1(18)	191.23	20.79	15.62	108.3	13.78
HF 2(30)	191.16	20.79	16.49	107.8	20.52
HF 3(30)	191.16	20.79	16.49	107.8	20.52
HF 4(38)	191.16	20.79	16.46	107.8	20.30
HF 5(36)	191.03	20.79	16.39	107.0	20.60
HF 6(44)	191.04	20.79	16.35	107.1	20.21
ωB97X-D 2(30)	191.95	24.96	13.44	110.2	6.30
ωB97X-D 3(30)	191.95	24.96	13.44	110.2	6.30
ωB97X-D 4(38)	191.95	24.96	13.40	110.1	6.34
ωB97X-D 5(36)	191.95	24.97	12.96	109.2	7.20
ωB97X-D 6(44)	191.95	24.97	12.95	109.2	7.22
ωB97X-D 7(44)	191.95	24.97	12.95	109.2	7.22
BP 2(30)	191.75	20.80	14.05	111.8	2.82
BP 3(30)	191.75	20.80	14.05	111.8	2.82
BP 4(38)	191.74	20.80	14.05	111.7	2.72
BP 5(36)	191.61	20.80	14.01	110.8	**1.55**
BP 6(44)	191.61	20.80	14.01	110.8	1.55
BP 7(44)	191.61	20.80	14.01	110.8	1.55
Experiment	191.59	20.82	14.11	109.8	0.00
Units	J/mol/K	J/mol/K	kJ/mol	pm	%

Legend. Orbital functions: 0(10) = STO-3G, 1(18) = 3-21G, 2(30) = 6-31G*, 3(30) = 6-31G**, 4(38) = 6-31+G*, 5(36) = 6-311G*, 6(44) = 6-311+G**, 7(44) = 6-311++G**. Methods (Spartan '14 software was used): HF–HF (Restricted Hartree–Fock); BP–DFT (Density Functional Theory), Exchange = Becke, Correlation = P86; ωB97X-D–DFT: Exchange = $0.222 \cdot H_F(LRC) + 1 \cdot \omega B97X - D(LRC)$, Correlation = wB97X-D. $\Delta r \leftarrow |Val_{Experiment} - Val_{Model}| / Val_{Experiment}$. Refs. for experiment data: S°, C_V in [43]; ZPE, d in [44].

Due to the simplicity of the composition (all Carbon atoms for cyclic polyynes; Carbon and Hydrogen atoms for linear polyynes, Boron, Carbon, and Nitrogen for {B,N}-congeners of cyclic polyynes appearing later in this study), the increasing complexity of the basis function, and sometimes of the theory level as well, does not provide further insights nor increase the accuracy of the modeling. One reference example for this is the calculations for a much well studied system, $N \equiv N$ molecule (Table 1).

Somebody may argue that DFT BP 6-311G* (BP 5 (36) in Table 1) is not enough. Let us take for instance [45] comment, which found B3LYP inappropriate for some C_{18} calculations; their main argument lies in a table pretty much alike our Table 1; anyway, since the method should be always a subject to change and improvement we should point our opinion that not always bigger is the better ("The ωB97XD functional with at least 6-311G(d) basis set" is suggested in [45]). To prove the contrary, in Table 1, the results for ωB97X-D were added as well.

3. Modeling

In order to reveal smaller amounts of variations, the average energy per atom (E/n) has been calculated (see Table 2). Furthermore, average energy per atom (or per bond) and bond lengths calculations for the formation of the polyyne rings (for $6 \leq n \leq 36$, even number) were conducted at different theory levels (including Hartree–Fock [46–49] and Becke–Perdew [50,51]), and three sets of results derived employing three methods were selected for discussion in this paper (see Table 2).

Table 2. Average energy per atom (E/n, a.u.) and distances between atoms ($d_{C,C}$, Å) for a single monocyclic ring polyyne (C_n), calculated at three different theory levels.

n	HF/STO-3G (Method M1)				HF/3-21G (Method M2)				BP/6-311G* (Method M3)			
	E/n	d_{C-C}	$d_{C\equiv C}$	Sym	E/n	d_{C-C}	$d_{C\equiv C}$	Sym	E/n	d_{C-C}	$d_{C\equiv C}$	Sym
6	−37.3083	1.2979	1.2979	D_{6h} [a]	−37.5767	1.2957	1.2957	D_{6h} [a]	−38.0492	1.3148	1.3148	D_{6h} [a]
8	−37.3268	1.4519	1.1948	C_{4h}	−37.5932	1.3955	1.2326	C_{4h}	−38.0599	1.3853	1.2703	C_{4h}
10	−37.3463	1.3893	1.2038	C_{5h}	−37.6103	1.3380	1.2215	C_{5h}	−38.0767	1.2944	1.2944	D_{10} [a]
12	−37.3522	1.4139	1.1902	C_{6h}	−37.6139	1.3831	1.1972	C_{6h}	−38.0746	1.3695	1.2383	C_{6h}
14	−37.3578	1.3986	1.1917	C_{7h}	−37.6194	1.3595	1.2029	C_{7h}	−38.0836	1.2896	1.2896	D_{14} [a,c]
16	−37.3606	1.4030	1.1884	C_{8h}	−37.6213	1.3699	1.1970	C_{8h}	−38.0816	1.3488	1.2436	C_{16} [d]
18	−37.3628	1.3988	1.1884	C_{9h}	−37.6235	1.3621	1.1987	C_{9h}	−38.0864	1.2879	1.2879	D_{18} [a,d]
20	−37.3643	1.3995	1.1872	C_{10}	−37.6247	1.3647	1.1967	C_{10}	−38.0849	1.3376	1.2477	C_{10}
22	−37.3654	1.3981	1.1870	C_{11}	−37.6258	1.3619	1.1972	C_{11}	−38.0878	1.2870	1.2870	D_{22} [a,e]
24	−37.3666	1.3980	1.1865	C_{12}	−37.6265	1.3625	1.1965	C_{12}	−38.0867	1.3305	1.2509	C_{12}
26	−37.3669	1.3975	1.1862	C_{13}	−37.6271	1.3614	1.1965	C_{13} [b]	−38.0886	1.2865	1.2865	D_{26} [a,f]
28	−37.3674	1.3973	1.1860	C_{14}	−37.6276	1.3614	1.1963	C_{14}	−38.0878	1.3256	1.2534	C_{14} [g]
30	−37.3678	1.3970	1.1858	C_{15}	−37.6280	1.3609	1.1962	C_{15}	−38.0891	1.2861	1.2861	D_{30} [a,h]
32	−37.3681	1.3969	1.1857	C_{16}	−37.6280	1.3713	1.1980	C_{16}	−38.0885	1.3222	1.2553	C_{16} [i]
34	−37.3684	1.3967	1.1855	C_{17}	−37.6285	1.3605	1.1961	C_{17}	−38.0894	1.2860	1.2860	D_{34} [a,j]
36	−37.3687	1.3966	1.1854	C_{18}	−37.6285	1.3726	1.1985	C_{18}	−38.0889	1.3192	1.2569	C_{18} [k]

Legend: [a] cumulene ($= C =$) is preferred over polyyne ($-C \equiv$); [b-k] symmetry is weaker, stdev(bond length) $> 5 \times 10^{-7}$: [b] 5×10^{-5}; [c] 3×10^{-5}; [d] 2×10^{-5}; [e] 5×10^{-5}; [f] 7×10^{-5}; [g] 3×10^{-5}; [h] 4×10^{-5}; [i] 1×10^{-5}; [j] 10×10^{-5}; [k] 0.5×10^{-5}.

Inspecting Table 2, one can see that it is in perfect agreement with the fact that, for C_6, the cumulene configuration is preferred (see the entry for $n = 6$ in Table 2). Hartree–Fock (HF) level of theory (methods M1 and M2 in Table 2) is the first (and the most simplistic) level of theory involving Schrädinger's equation (the wave function of the quantum-mechanical system [52]). For this reason is not only scholastic, but also informative to reveal tendencies in stability (see BH&H functional in [53]), to inspect the dependencies using data retrieved from the modelling at this level of theory. Thus, in order to reveal the evolution of the stability, the data from Hartree–Fock (*HF*) levels of theory (M1 and M2 in Table 2) was plotted against the number of atoms (*n*) in Figure 2. Both dependencies show an increase in stability for $n \geq 6$ with the increase of *n*. However, the increase is decaying with the increase of *n* and it reaches about 95% of it for $n = 24$. Furthermore, stability increases in a decaying manner, while decay is most likely hyperbolic (see Equations (1) and (2)).
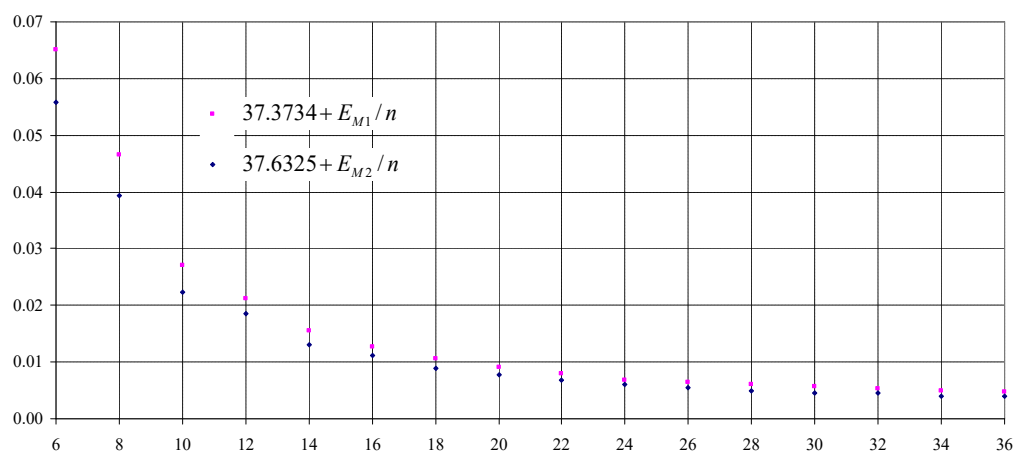
Figure 2. Average energy per atom (E/n, from M1, and M2, in a.u.) as function of number of atoms (*n*, even numbers from 6 to 36).

Two equations with a great likelihood were identified for HF energy per atom (Equations (1) and (2)). Both equations reveal an asymptotic convergence to infinity as well as a vertical asymptote in $n = 5$. What is intriguing is the appearance of the $n = 5$ vertical asymptote, and it can be associated with the nonexistence in normal conditions of cyclopentadienyl as neutral molecule, only as an anion [54], stabilized typically by the presence of an electron transferring element such as is Fe [55,56]. It should be noticed that there is a bump in symmetry for C_{26} (see Table 2, entry for $n = 26$). Employing a significantly different theory level with a notable increase in the number of orbital functions as well (M3 is a Density Functional Theory (DFT) method and is chosen as being the most accurate alternative for $N \equiv N$; see Table 1), polyyne is no longer preferred over cumulene almost anywhere, and modeling reveals an alternation between these two configurations, cumulenes being preferred when n is a multiple of two but not a multiple of four ($n = 4k + 2$, with a D_{nh} symmetry) and polyynes when n is a multiple of four ($n = 4k$, with a $C_{\frac{n}{2}h}$ symmetry).

$$\hat{E}_{M1}/n = \frac{-37.3734_{\pm 2}n + 187.007_{\pm 5}}{n - 5} \text{ (a.u.), } r^2_{adj.} = 0.9984 \tag{1}$$

$$\hat{E}_{M2}/n = \frac{-37.6325_{\pm 5}n + 188.280_{\pm 7}}{n - 5} \text{ (a.u.), } r^2_{adj.} = 0.9956 \tag{2}$$

$$\hat{E}_{M3}/n = \frac{-38.0932_{\pm 6}n + 114.441_{\pm 9}}{n - 3} \text{ (a.u.), } r^2_{adj.} = 0.993, n = 4k \tag{3}$$

$$\hat{E}_{M3}/n = \frac{-38.0932_{\pm 6}n + 152.462_{\pm 5}}{n - 4} \text{ (a.u.), } r^2_{adj.} = 0.993, n = 4k + 2 \tag{4}$$

When $n \leftarrow 4k$, we obtain equations for polyynes and when $n \leftarrow 4k + 2$ for cumulenes.

3.1. Unusual Regression for C_n Polyyne/Cumulene Energy (Equations (3) and (4))

If one constructs a regression with E/n as function ($\hat{y} = \hat{y}(x)$) of n for polyynes ($n = 4k, k = 1, 2, \ldots$), it will get with a high confidence that in $\hat{y}(x) = (a_0 + a_1 x)/(x - a_2)$, $a_2 = 3$ (see Equation (3)), just like $a_2 = 5$ in Equation (1) and (2). Thus, to solve the regression equation for polyynes, it is necessary to estimate a_0 and a_1 parameters from $\hat{y}(x) = (a_0 + a_1 x)/(x - 3)$. Following the same reasoning, to solve the regression equation for cumulenes, it is necessary to estimate b_0 and b_1 parameters from $\hat{z}(x) = (b_0 + b_1 x)/(x - 4)$. With increase of the number of atoms (n) the change in the energy per atom (E/n) must (and it, as Figure 2, reveals as well) become smaller, so, in convergence ($n \to \infty$), both formulas should express the same. Thus, $\lim_{x \to \infty} \hat{y}(x) = a_1 = b_1 = \lim_{x \to \infty} \hat{z}(x)$. Let us consider a series of values (such as is E/n in Table 2) associated with and corresponding to the increasing values of n for which the regression analysis has revealed that the model estimating values in the series have an alternating pattern, such as is the one provided in Equations (3) and (4):

$$y \sim \hat{y} = \frac{a_0 + a_1 x}{x - 3}, \text{ for } x \leftarrow n = 4k \ (n = 8, 12, \ldots, 36)$$

and

$$z \sim \hat{z} = \frac{b_0 + b_1 x}{x - 4}, \text{ for } x \leftarrow n = 4k + 2 \ (n = 6, 10, \ldots, 34)$$

In order to find the values of the parameters of the regression equations under a constraint: $a_1 = b_1$ (let us set $c_0 \leftarrow a_1 = b_1$), the following sum must be minimized:

$$S(a_0, b_0, c_0) = \sum_{k=2}^{9} (a_0 + c_0 w_k - t_k)^2 + \sum_{k=2}^{9} (b_0 + c_0 v_k - u_k)^2$$

where $t_k \leftarrow y_k(4k - 3)$, $u_k \leftarrow z_k(4k - 6)$, $v_k \leftarrow (4k - 2)$ and $w_k \leftarrow 4k$ substitutions are used for simplification here and from hereon.

The result is a linear and homogenous system with three equations and three variables and the variances are to be obtained by inversing the Fisher Information Matrix [57]:

$$
\begin{cases}
\sum\limits_{k=2}^{9} t_k = a_0 \sum\limits_{k=2}^{9} 1 + c_0 \sum\limits_{k=2}^{9} w_k \\
\sum\limits_{k=2}^{9} u_k = b_0 \sum\limits_{k=2}^{9} 1 + c_0 \sum\limits_{k=2}^{9} v_k \\
\sum\limits_{k=2}^{9} t_k w_k + v_k u_k = a_0 \sum\limits_{k=2}^{9} w_k + b_0 \sum\limits_{k=2}^{9} v_k + c_0 \left(\sum\limits_{k=2}^{9} w_k^2 + \sum\limits_{k=2}^{9} v_k^2 \right)
\end{cases}
$$

from which c_0 is

$$
c_0 = \frac{\sum\limits_{k=2}^{9} 1 \sum\limits_{k=2}^{9} w_k t_k + v_k u_k - \sum\limits_{k=2}^{9} w_k \sum\limits_{k=2}^{9} t_k - \sum\limits_{k=2}^{9} v_k \sum\limits_{k=2}^{9} u_k}{\sum\limits_{k=2}^{9} 1 \left(\sum\limits_{k=2}^{9} w_k^2 + \sum\limits_{k=2}^{9} v_k^2 \right) - \left(\sum\limits_{k=2}^{9} w_k \right)^2 - \left(\sum\limits_{k=2}^{9} v_k \right)^2}
$$

and a_0 and b_0 are subsequently immediate (from first two equations of the system).

3.2. Further Deriving of Regression Equations

All obtained Equations (1)–(4) are statistically significant. It is in fact surprising how accurate the obtained models are (the precision digit, given for a 5% risk of being in error is the 6th digit everywhere), considering the small size of the data analyzed. It is interesting how the average energy per atom has a vertical asymptote at $n = 3$ for the polyynes (see Equation (3)) and a vertical asymptote at $n = 4$ for the cumulenes (see Equation (4)), and this behavior warrants further investigation.

The distances between atoms (columns d_{C-C} and $d_{C\equiv C}$ in Table 2) are in any circumstance, independently of the model, at least smaller, stronger than the aromatic bond (1.385 Å). Expected to be a more accurate model, BP/6-311G* reveals (Equations (5)–(7)) a convergence of the cumulene bond length to the average of the polyyne bond length ($1.281 = (1.295 + 1.267)/2$).

$$
\hat{d}_{C-C,M3} = 1.295_{\pm 1} + 0.87_{\pm 3}/n \ (\text{Å}), r^2_{adj.} = 0.999, \text{polyynes} \tag{5}
$$

$$
\hat{d}_{C\equiv C,M3} = 1.267_{\pm 2} - 0.36_{\pm 3}/n \ (\text{Å}), r^2_{adj.} = 0.999, \text{polyynes} \tag{6}
$$

$$
\hat{d}_{C=C,M3} = 1.281_{\pm 2} + 0.11_{\pm 1}/n \ (\text{Å}), r^2_{adj.} = 0.999, \text{cumulenes} \tag{7}
$$

Equations (5)–(7) were obtained following the same regression strategy as for Equations (3) and (4) (see Section 3.1). Consistent with the energy assessment (about 5% of the stabilizing energy lost due to bending, as seen above), the C_{24} polyyne bonds lengths are about 2% different than the limit values (single bond is about 2.7% longer, triple bond is about 1.3% shorter, as seen by the data in Table 2 and Equations (5) and (6)), making it a very good candidate for stabilization by condensation.

4. Constructing Molecular Rings

4.1. Constructing a Polyyne Ring

A polyyne ring is characterized by the alternating of single and triple bonds which corresponds to an even-number sided polygon. A good starting geometry places the nucleus of atoms on a circle of a certain radius (r) at alternating distances corresponding to single (b_1) and triple (b_3) bonds lengths. Assuming that AB is the triple bond (of length b_3), BC is the single bond (of length b_1) and OA is the radius (r) of the circumscribed circle (see Figure 3), then using AOC = AOB + BOC and expressing the angles (AOB = 2arcsin(b_1/r), BOC = 2arcsin(b_3/r) and AOC = $4\pi/n$), the result is a rather difficult one to be resolved directly with equation:
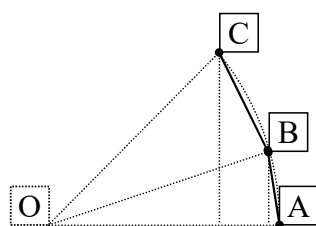
Figure 3. Auxiliary representation for constructing a polyyne ring.

$$\sin\left(\frac{4\pi}{n}\right) = \left(1 - 2\left(\frac{b_1}{2r}\right)^2\right)\frac{b_3}{2r}\sqrt{1 - \left(\frac{b_3}{2r}\right)^2} + \left(1 - 2\left(\frac{b_3}{2r}\right)^2\right)\frac{b_1}{2r}\sqrt{1 - \left(\frac{b_1}{2r}\right)^2}$$

A simpler choice is using a program to obtaiin the radius (r) through successive approximations:

$$\left[\; u \leftarrow \arcsin\left(\frac{b_3}{2r}\right); v \leftarrow \arcsin\left(\frac{b_1}{2r}\right); r \leftarrow \frac{b_1\cos\left(u + \frac{v}{2}\right) + b_3\cos\left(\frac{u}{2}\right)}{\sin\left(\frac{4\pi}{n}\right)} \;\right]_i$$

Starting with a rough approximation (this approximation gets closer to the exact solution with the increase of n): $r \leftarrow (b_1 + b_3)/\sin(4\pi/n)$ the iterations ($i \leftarrow 1, 2, \ldots$) converge on the exact solution leaving a residual below 10^{-8} in 18 iterations for $n = 6$ and in six iterations for $n = 36$.

4.2. C_{24} Ring and Its {B,N}-Congeners

C_{24} ring is very likely to stabilize the polyyne bonds (only about 5% of the energy increase is lost by the bending, as seen in Figure 2 and Equation (3); it is the biggest polyyne with unaltered symmetry, as seen in Table 2; bond lengths have very few differences (about 2%, see Equations (5)–(7)) to the limit infinite chain values). Previous reports [18,31] also show its potential from other perspectives.

Of interest is the substitution of Carbon atoms with Nitrogen and Boron in a regular, patterned manner [38]. Numerous congeners of carbon-based materials have been reported following such substitution [58], including inorganic benzene [59], boron nitride [60], nanotubes [61] and graphene-like materials [62].

Here, alternating between Boron and Nitrigen ($B_{12}N_{12}$) and between Boron, Carbon and Nitrogen ($C_8B_8N_8$) congeners of C_{24} have been designed, and their properties have been calculated and analyzed at BP/6-311G* level of theory (therefore with $M3$).

Raman along with Infrared (IR) spectroscopy is commonly (in both organic and inorganic chemistry, in research and industry) used to provide a structural fingerprint by which molecules can be identified since is a simple and reliable technique [63–65]. Some molecular vibrational motions are associated with certain bonds or bonding environments or atoms groups, while others involve movement of almost all of the atoms in the molecule, being characteristic of the molecule as a whole. It is possible to calculate the vibrational frequencies associated with IR spectra, by using the data from quantum mechanics calculations. The nuclei are assumed to move much more slowly than the electrons, which are much lighter and thus more mobile. In this limit, the nuclei are assumed to move within an internuclear potential energy surface that is generated by the electrons (Born–Oppenheimer approximation [66]), and is accurate within fractions of a percent [67]. The calculation is based on optimal nucleus positions and electronic densities involving the evaluation of the electronic magnetic moment derivatives as detailed in [68].

Because vibrational frequencies are specific to a molecule's chemical bonds and symmetry, the RAMAN spectra are also of interest (see Figure 4), where there is prominent one major peak shifting in the spectra.
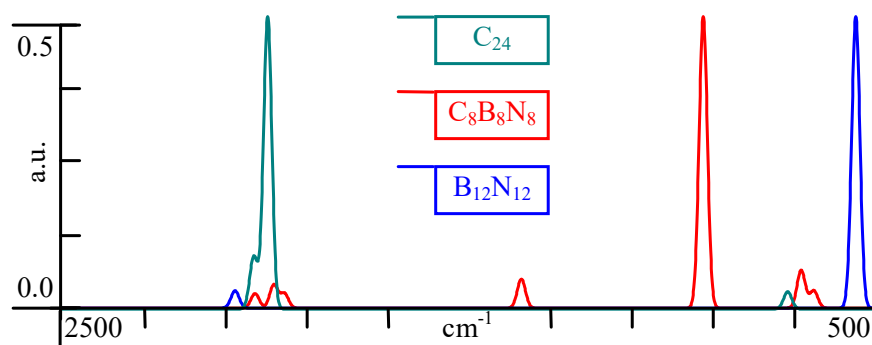
Figure 4. Calculated RAMAN spectra of C_{24} congeners.

Substituting the Carbon atoms with Boron and Nitrogen produces a shift in the RAMAN spectra, but since it is only one major peak, it keeps the symmetry at a comparable level everywhere.

Fundamental vibrations and associated rotational-vibrational structures are revealed by the IR spectra (see Figure 5).
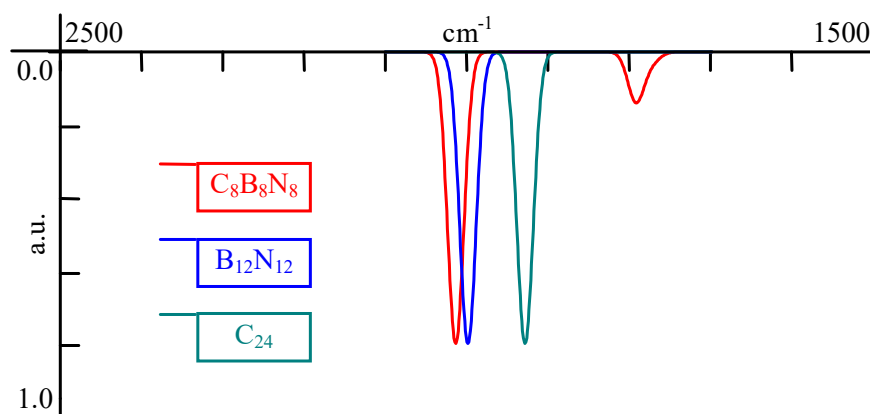
Figure 5. Calculated IR spectra of C_{24} congeners: zoom in into the region of interest ([2500 cm^{-1}, 1500 cm^{-1}]) for the mid-infrared spectra.

Substituting the Carbon atoms with Boron and Nitrogen produces a small shift in the IR spectra in the case of $B_{12}N_{12}$ and also a small absorption peak appears in the case of $C_8B_8N_8$. There is no symmetry reduction from C_{24} (C_{12} point group symmetry; atom coordinates in Table A1) to $B_{12}N_{12}$ (D_{12} point group symmetry; atom coordinates in Table A2) explainable by the tilting from polyyne (1.251 Å and 1.331 Å as bond lengths) to cumulene (1.321 Å bond length) bonds. It should be noted that, even if the Carbon atoms in C_{24} are located on two circles (alternating), these have approximately the same radius (4.9441 Å and 4.9444 Å) but in the case of $B_{12}N_{12}$ Boron atoms are accommodated on an interior circle (of 4.921 Å radius) significantly distinct from the exterior one (of 5.103 Å radius) accommodating Nitrogen atoms. Even more intriguing is the case of $C_8B_8N_8$ with C_{4h} point group symmetry (Figures 6 and 7).

In Figure 6, the radiuses (in Å) are as follows (in ascending order, from interior to exterior):

- Conformer 1: 4.998 (B), 5.006 (N), 5.012 (C), 5.018 (C), 5.064 (N), 5.145 (B);
- Conformer 2: 4.994 (B), 5.004 (C), 5.017 (N), 5.045 (C), 5.046 (N), 5.140 (B).
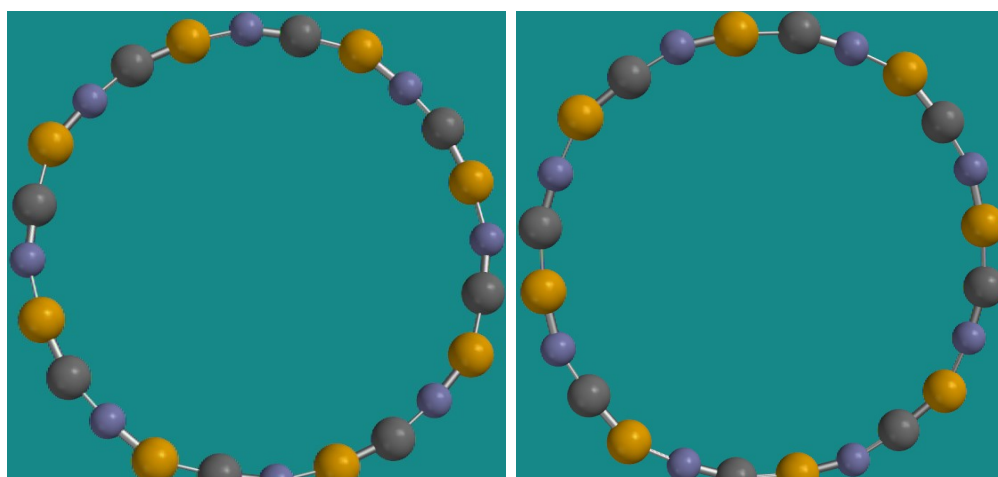
Figure 6. Spartan '14 images for the two conformers of $C_8B_8N_8$ (atoms coordinates in Table A3 and Table A4, respectively).

Since the differences between radiuses are very small, in order to illustrate more clearly the differences, Figure 7 represents the same conformers with the geometry not to scale. In Figure 7, it is visible that, while the inner ring is formed by the Boron atoms in both conformers (green balls in Figure 7), the next two interior rings are formed by Nitrogen and then Carbon for Conformer 1, while, in Conformer 2, the ring of Carbon appears next followed by the ring of Nitrogen.
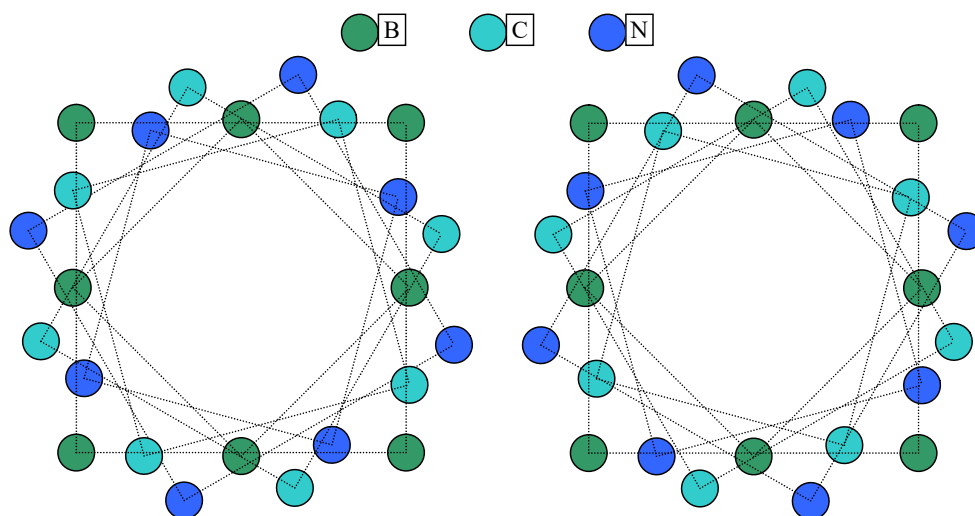
Figure 7. The two conformers of $C_8B_8N_8$ (not to scale; C_{4h} point group symmetry).

Regarding other properties of C_{24} polyyne congeners calculated from the molecular modeling (DFT M3) and listed in Table 3, one should notice very little change in entropy from C_{24} to $B_{12}N_{12}$ and the very small HOMO-LUMO gap of $C_8B_8N_8$ (which, coupled with greatest heat capacity and smallest zero point energy, deems it a very interesting subject for further studies). The decrease of polarizability of $B_{12}N_{12}$ relative to C_{24} is conjugated with the increase of HOMO-LUMO gap to a value (4 eV) at limit when the near-degeneracy can be removed and the HOMO stabilized by distortion to a lower symmetry structure that brings about electron occupancy of the LUMO [69].

Table 3. Calculated properties of C_{24} congeners (with DFT M3).

Property	$C_8B_8N_8$	$B_{12}N_{12}$	C_{24}
HOMO (eV)	−4.76	−6.55	−5.55
LUMO (eV)	−4.73	−2.55	−4.88
Polarizability (10^{-30}m^3)	69.12	67.77	69.22
C_v (J/mol°K)	229.36	227.12	224.80
ZPE (kJ/mol)	266.05	280.91	295.12
S° (J/mol°K)	590.53	556.27	556.98
H° (au)	−941.545940	−956.058936	−913.947924
G° (au)	−941.613001	−956.122105	−914.011174
Energy (au)	−941.668686	−956.185626	−914.080632

HOMO and LUMO—highest occupied and lowest unoccupied molecular orbitals; Polarizability—calculated using the method reported in [70]; ZPE—zero point energy; S, H, and G—entropy, enthalpy, and free enthalpy.

The bond lengths in $B_{12}N_{12}$ (1.32 Å) are smaller than a typical Carbon-Carbon double bond (1.34 Å) suggesting that $B_{12}N_{12}$ has a very good potential to make compact, hard materials. In the case of $C_8B_8N_8$, the bond length between Boron and Carbon (1.38 Å and 1.41 Å, alternating) suggests presence of the aromaticity (1.385 Å is the typical length of the aromatic bond in benzene), while the bond length between Boron and Nitrogen (1.31 Å and 1.34 Å, alternating) suggests the presence of at least a double bond (typical Carbon - Carbon double bond length is 1.34 Å) while the bond length between Carbon and Nitrogen (1.22 Å and 1.24 Å, alternating) indicates an intermediate strength between a double (1.28 Å is the typical length of the double bond between Carbon and Nitrogen) and a triple bond (1.16 Å is the typical length of the triple bond between Carbon and Nitrogen).

5. Molecular Clusters

A molecular mechanics method [18] was involved in minimizing the energies of clusters, while $4C_{24}$ polyyne cluster and $4B_{12}N_{12}$, $4C_{26}$, and $4B_{13}N_{13}$ cumulene and cumulene-like cluster structures were further optimized at Hartree–Fock theory level using 6-311G* basis set [71]. Two different conformations were identified (see Figure 8).
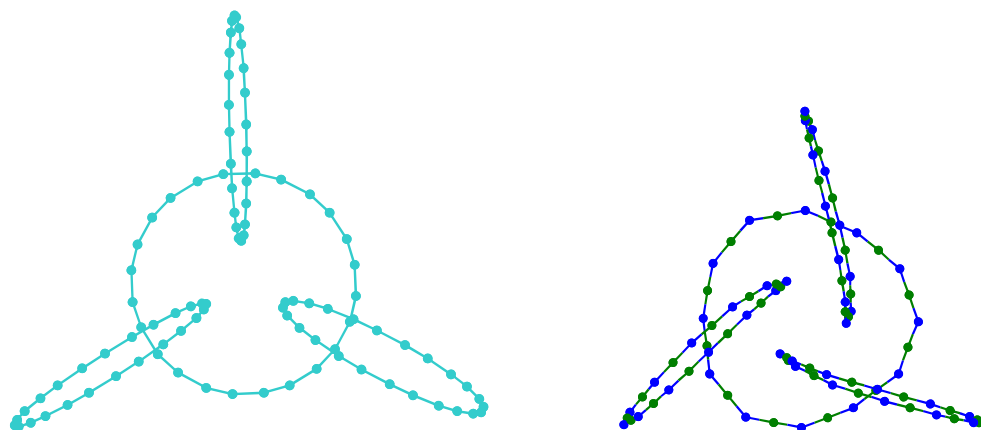
Figure 8. Conformation of $4C_{24}$ polyyne (image to the **left**) and $4B_{12}N_{12}$ cumulene (image to the **right**) clusters (models from HF/6-311G* geometry, atom coordinates in Tables A5 and A6).

Cumulene conformation (build up from alternating Boron and Nitrogen) has an increased entropy (the geometry is more irregular and the outer rims are bended), suggesting that a longer circle length is stabilizing.

The result is consistent with previously reported data [18]. One different aspect: here, involving an upper theory level in the final geometry optimization, one can distinguish between the geometry of the polyyne Figure 8 left—preferring an axial alignment of the outer rims and the geometry of the cumulene Figure 8 right—preferring a paddle alignment of the outer rims.

The $4C_{24}$ polyyne (Figure 8 left) has, in its geometrically optimized form (using HF 6-311G*), an entirely symmetrical form: the outer rims are perfectly perpendicular to the inner rim (90° between the versors of their planes) and the angles between the planes of the outer rims are, again, in a perfect symmetry (120° between them), the $4C_{24}$ polyyne cluster having a D_{3h} molecular point group. The $4B_{12}N_{12}$ cumulene (Figure 8 right) has a small break in its symmetry—the angles of the outer rims with the inner rim are a little bigger (90.1°), the angles between the outer rims are a little smaller (117.2°), and the plane of their centers does not include the center of the inner rim (this is off by 0.023 Å). More importantly, the centers of the outer rims are significantly closer to the center of the inner rim in the case of the $4B_{12}N_{12}$ cumulene (4.969 Å) when compared with the $4C_{24}$ polyyne (6.755 Å).

Figure 9 gives a picture of the $4C_{24}$ polyyne cluster in its final, optimized conformation depicting the electronic density.
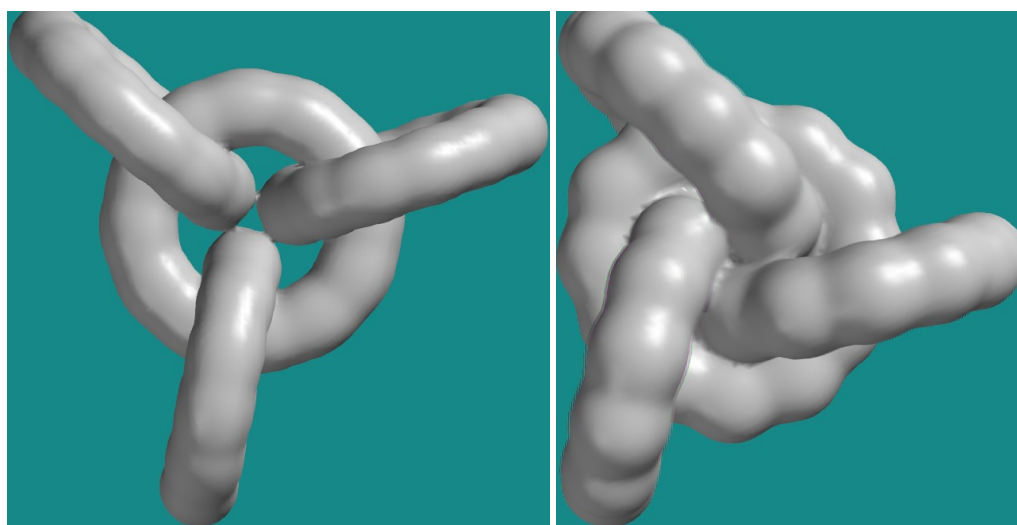
Figure 9. Electronic density and electrostatic potential map—those two have essentially the same shape-of $4C_{24}$ polyyne cluster (image to the **left**) and of $4B_{12}N_{12}$ cumulene (image to the **right**)-Spartan '14 screen captures.

In the case of the $4C_{24}$ polyyne cluster, the electronic density distribution reveals a natural accommodation of the crosses-no overlap and no gap between the 95% coverage of the electronic density, no bending due to the crossing. In the case of the $4B_{12}N_{12}$ cumulene, the electronic density distribution reveals a very good occupancy of the space inside of the inner rim by the 95% coverage of the electronic density suggesting a configuration stress.

Furthermore, the optimized geometry of $4C_{26}$ cumulene (Figure 10) proves the fact that $4C_{24}$ polyyne (Figure 8 left) is the optimal conformation, having a balanced use of the free space.

$4C_{26}$ cumulene conformers reveal the existence of extra free space in their conformation. In the image to the left, the outer rims are not perfectly vertical (being positioned at 85.0°, 85.2°, and 86.2°, respectively, relative to the inner circle). The angles between the outer rims are 106.9°, 124.6°, and 126.7°, respectively. In the image to the right, the vertical alignment is improved (91.1°, 91.3°, and 92.3° respectively) but the departure to the perfect symmetry (angles of 120°) is pushed even further away (107.9°, 121.7°, and 130.1°, respectively).
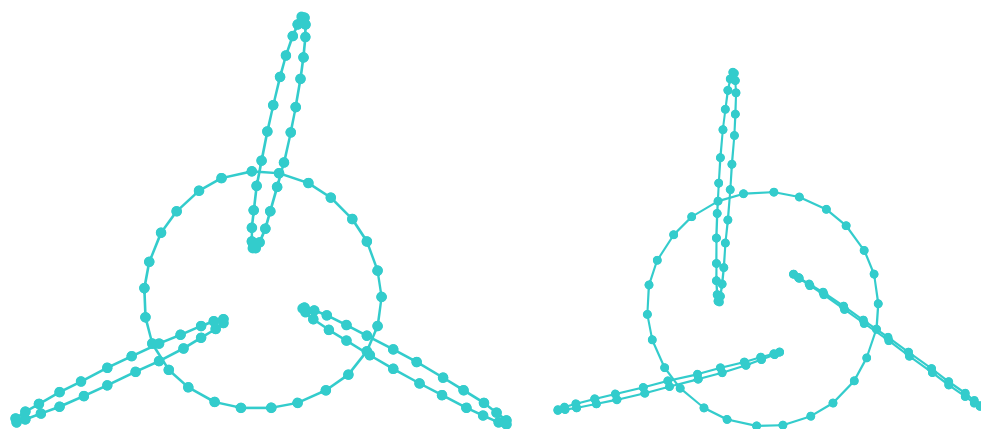
Figure 10. Optimal geometry of $4C_{26}$ cumulene conformers (models from HF/6-311G* geometry, atoms coordinates in Tables A7 and A8 respectively).

6. Conclusions

Polyynes, possessing metallic and semiconducting properties, and susceptible for valuable superconductivity, are also very attractive for applications requiring dense materials with very good compressibility. Energy and conformation analyses employed in this study at different theory levels (including HF and DFT) revealed that cyclic conformation begins to stabilize itself for medium sized rings, having an optimum (characterized by only a 5% energy loss due to bending) at $n = 24$ atoms. Polyyne conformations (alternations of single-like and triple-like bonds) are preferred by Carbon rings of sizes that are multiples of 4 (…, 16, 20, 24, 28, 32, …) while cumulene conformations are preferred for the rest of the cases (Carbon rings of sizes that are non-multiples of 4 (…, 18, 22, 26, 30, …) and alternations of Boron and Nitrogen atoms ($B_{12}N_{12}$ studied here). The bond length split present at $C_8B_8N_8$ (bond length between Boron and Carbon is 1.38 Å and 1.41 Å, alternating; bond length between Boron and Nitrogen is 1.31 Å and 1.34 Å, alternating; bond length between Carbon and Nitrogen is 1.22 Å and 1.24 Å, alternating) as well as the lengths of these bonds indicate an intermediate configuration (between polyyne and cumulene) which warrants further study. The existence of the polyyne and/or cumulene long chain is further stabilized when molecular clusters are formed. The analysis of $4C_{24}$, $4B_{12}N_{12}$, $4C_{26}$, and $4B_{13}N_{13}$ clusters (all built on a cluster topology in which one central ring is crossed by other three rings) revealed that $4C_{24}$ polyyne and $4B_{12}N_{12}$ cumulene are [4]catenane arrangements that are best balancing the free space between atoms.

Conflicts of Interest: The author declares no conflict of interest.

Appendix A

Table A1. Cartesian coordinates of C_{24} cyclic cumulene having DFT BP 6-311G* optimal geometry.

4.78618	−1.24089	0	4.94409	0.00000	0	4.76540	1.31845	0	4.28171	2.47205	0
3.46773	3.52451	0	2.47205	4.28171	0	1.24089	4.78618	0	0.00000	4.94409	0
−1.31845	4.76540	0	−2.47205	4.28171	0	−3.52451	3.46773	0	−4.28171	2.47205	0
−4.78618	1.24089	0	−4.94409	0.00000	0	−4.76540	−1.31845	0	−4.28171	−2.47205	0
−3.46773	−3.52451	0	−2.47205	−4.28171	0	−1.24089	−4.78618	0	0.00000	−4.94409	0
1.31845	−4.76540	0	2.47205	−4.28171	0	3.52451	−3.46773	0	4.28171	−2.47205	0

Table A2. Cartesian coordinates of $B_{12}N_{12}$ cyclic cumulene having DFT BP 6-311G* optimal geometry.

3.79257	3.41407	0	2.68051	4.12673	0	1.57740	4.85298	0	0.25800	4.91411	0
−1.06039	4.99150	0	−2.23359	4.38476	0	−3.41411	3.79256	0	−4.12675	2.68049	0
−4.85296	1.57742	0	−4.91411	0.25803	0	−4.99151	−1.06042	0	−4.38475	−2.23362	0
−3.79257	−3.41407	0	−2.68051	−4.12673	0	−1.57740	−4.85298	0	−0.25800	−4.91411	0
1.06039	−4.99150	0	2.23359	−4.38476	0	3.41411	−3.79256	0	4.12675	−2.68049	0
4.85296	−1.57742	0	4.91411	−0.25803	0	4.99151	1.06042	0	4.38475	2.23362	0

Table A3. Cartesian coordinates of C_{24} cyclic cumulene conformer 1 having DFT BP 6-311G* optimal geometry.

3.62802	−3.64575	0	4.37263	−2.44972	0	4.88467	−1.33917	0	4.99818	0.00000	0
4.82863	1.36764	0	4.33202	2.50870	0	3.64575	3.62802	0	2.44972	4.37263	0
1.33917	4.88467	0	0.00000	4.99818	0	−1.36764	4.82863	0	−2.50870	4.33202	0
−3.62802	3.64575	0	−4.37263	2.44972	0	−4.88467	1.33917	0	−4.99818	0.00000	0
−4.82863	−1.36764	0	−4.33202	−2.50870	0	−3.64575	−3.62802	0	−2.44972	−4.37263	0
−1.33917	−4.88467	0	0.00000	−4.99818	0	1.36764	−4.82863	0	2.50870	−4.33202	0

Table A4. Cartesian coordinates of C_{24} cyclic cumulene conformer 2 having DFT BP 6-311G* optimal geometry.

4.33233	−2.50908	0	4.82779	−1.36740	0	4.99764	0.00000	0	4.88379	1.33938	0
4.37257	2.45010	0	3.62884	3.64692	0	2.50908	4.33233	0	1.36740	4.82779	0
0.00000	4.99764	0	−1.33938	4.88379	0	−2.45010	4.37257	0	−3.64692	3.62884	0
−4.33233	2.50908	0	−4.82779	1.36740	0	−4.99764	0.00000	0	−4.88379	−1.33938	0
−4.37257	−2.45010	0	−3.62884	−3.64692	0	−2.50908	−4.33233	0	−1.36740	−4.82779	0
0.00000	−4.99764	0	1.33938	−4.88379	0	2.45010	−4.37257	0	3.64692	−3.62884	0

Table A5. Cartesian coordinates of $4C_{24}$ cyclic cumulene having HF 6-311G* optimal geometry.

−1.91612	4.70183	0.00000	−3.11384	4.01033	0.00000	−3.90083	3.11278	0.00000	−4.48926	1.86180	0.00000
−4.72452	0.69121	0.00000	−4.72452	−0.69121	0.00000	−4.48926	−1.86180	0.00000	−3.90083	−3.11278	0.00000
−3.11384	−4.01033	0.00000	−1.91612	−4.70183	0.00000	−0.74533	−4.93461	0.00000	0.63227	−4.81871	0.00000
1.76366	−4.43716	0.00000	2.96087	−3.74595	0.00000	3.85699	−2.95692	0.00000	4.64617	−1.82183	0.00000
5.02997	−0.69150	0.00000	5.02997	0.69150	0.00000	4.64617	1.82183	0.00000	3.85699	2.95692	0.00000
2.96087	3.74595	0.00000	1.76366	4.43716	0.00000	0.63227	4.81871	0.00000	−0.74533	4.93461	0.00000
1.90890	0.00000	0.68777	1.90890	0.00000	−0.68777	2.20706	0.00000	−1.84016	2.88387	0.00000	−3.03723
3.72300	0.00000	−3.88360	4.91360	0.00000	−4.57357	6.06469	0.00000	−4.88178	7.44086	0.00000	−4.87949
8.59115	0.00000	−4.56844	9.78112	0.00000	−3.87716	10.62161	0.00000	−3.03250	11.30748	0.00000	−1.83940
11.61471	0.00000	−0.68810	11.61471	0.00000	0.68810	11.30748	0.00000	1.83940	10.62161	0.00000	3.03250
9.78112	0.00000	3.87716	8.59115	0.00000	4.56844	7.44086	0.00000	4.87949	6.06469	0.00000	4.88178
4.91360	0.00000	4.57357	3.72300	0.00000	3.88360	2.88387	0.00000	3.03723	2.20706	0.00000	1.84016
−3.03235	−5.25218	−4.88178	−3.72043	−6.44398	−4.87949	−4.29558	−7.44015	−4.56844	−4.89056	−8.47070	−3.87716
−5.31081	−9.19859	−3.03250	−5.65374	−9.79256	−1.83940	−5.80735	−10.05863	−0.68810	−5.80735	−10.05863	0.68810
−5.65374	−9.79256	1.83940	−5.31081	−9.19859	3.03250	−4.89056	−8.47070	3.87716	−4.29558	−7.44015	4.56844
−3.72043	−6.44398	4.87949	−3.03235	−5.25218	4.88178	−2.45680	−4.25530	4.57357	−1.86150	−3.22421	3.88360
−1.44193	−2.49750	3.03723	−1.10353	−1.91137	1.84016	−0.95445	−1.65315	0.68777	−0.95445	−1.65315	−0.68777
−1.10353	−1.91137	−1.84016	−1.44193	−2.49750	−3.03723	−1.86150	−3.22421	−3.88360	−2.45680	−4.25530	−4.57357
−5.65374	9.79256	1.83940	−5.31081	9.19859	3.03250	−4.89056	8.47070	3.87716	−4.29558	7.44015	4.56844
−3.72043	6.44398	4.87949	−3.03235	5.25218	4.88178	−2.45680	4.25530	4.57357	−1.86150	3.22421	3.88360
−1.44193	2.49750	3.03723	−1.10353	1.91137	1.84016	−0.95445	1.65315	0.68777	−0.95445	1.65315	−0.68777
−1.10353	1.91137	−1.84016	−1.44193	2.49750	−3.03723	−1.86150	3.22421	−3.88360	−2.45680	4.25530	−4.57357
−3.03235	5.25218	−4.88178	−3.72043	6.44398	−4.87949	−4.29558	7.44015	−4.56844	−4.89056	8.47070	−3.87716
−5.31081	9.19859	−3.03250	−5.65374	9.79256	−1.83940	−5.80735	10.05863	−0.68810	−5.80735	10.05863	0.68810

Table A6. Cartesian coordinates of $4B_{12}N_{12}$ cyclic cumulene having HF 6-311G* optimal geometry.

−1.76825	4.36002	−0.01740	−3.04477	4.06970	−0.01277	−3.92879	3.10051	−0.01653	−4.83161	2.15186	−0.01709
−4.93518	0.84670	−0.01869	−5.00212	−0.45994	−0.01947	−4.41697	−1.62735	−0.01976	−3.80821	−2.78179	−0.01951
−2.89176	−3.71136	−0.01740	−2.00208	−4.67170	−0.01277	−0.72072	−4.95269	−0.01653	0.55224	−5.26023	−0.01709
1.73433	−4.69734	−0.01869	2.89938	−4.10199	−0.01947	3.61781	−3.01153	−0.01976	4.31321	−1.90711	−0.01951
4.66002	−0.64866	−0.01740	5.04685	0.60200	−0.01277	4.64951	1.85218	−0.01653	4.27937	3.10837	−0.01709
3.20085	3.85064	−0.01869	2.10274	4.56193	−0.01947	0.79916	4.63888	−0.01976	−0.50499	4.68890	−0.01951
0.45557	−1.95282	1.12465	0.07075	−1.97729	−0.12663	0.52155	−1.93908	−1.35625	0.91464	−1.93971	−2.59202
1.82698	−1.71765	−3.50609	2.72566	−1.51437	−4.41968	3.91641	−1.06917	−4.72814	5.09941	−0.63335	−5.04421
6.25905	−0.16813	−4.66280	7.41781	0.29606	−4.29618	8.23877	0.63337	−3.33902	9.07144	0.97414	−2.39785
9.34014	1.08722	−1.12658	9.63091	1.20674	0.13815	9.27914	1.06213	1.38456	8.94865	0.92424	2.63883
8.07121	0.56300	3.53033	7.20429	0.20475	4.43813	6.02906	−0.26606	4.73741	4.85237	−0.73905	5.05123
3.68354	−1.16113	4.67110	2.50644	−1.59451	4.29879	1.65198	−1.77217	3.33893	0.78031	−1.97173	2.38048
−2.88414	−2.85712	−4.72814	−3.09820	−4.09955	−5.04421	−3.27513	−5.33643	−4.66280	−3.45251	−6.57205	−4.29618
−3.57087	−7.45167	−3.33902	−3.69209	−8.34316	−2.39785	−3.72851	−8.63241	−1.12658	−3.77038	−8.94398	0.13815
−3.71974	−8.56704	1.38456	−3.67391	−8.21188	2.63883	−3.54803	−7.27137	3.53033	−3.42482	−6.34147	4.43813
−3.24495	−5.08829	4.73741	−3.06622	−3.83275	5.05123	−2.84734	−2.60948	4.67110	−2.63411	−1.37339	4.29879
−2.36074	−0.54457	3.33893	−2.09772	0.31010	2.38048	−1.91898	0.58187	1.12465	−1.74776	0.92738	−0.12663
−1.94007	0.51787	−1.35625	−2.13716	0.17776	−2.59202	−2.40102	−0.72339	−3.50609	−2.67431	−1.60331	−4.41968
−5.55940	7.50491	1.38456	−5.27474	7.28764	2.63883	−4.52318	6.70837	3.53033	−3.77947	6.13672	4.43813
−2.78412	5.35435	4.73741	−1.78615	4.57179	5.05123	−0.83621	3.77061	4.67110	0.12767	2.96790	4.29879
0.70876	2.31674	3.33893	1.31741	1.66163	2.38048	1.46341	1.37095	1.12465	1.67701	1.04992	−0.12663
1.41852	1.42121	−1.35625	1.22252	1.76196	−2.59202	0.57404	2.44104	−3.50609	−0.05135	3.11768	−4.41968
−1.03227	3.92630	−4.72814	−2.00121	4.73289	−5.04421	−2.98392	5.50457	−4.66280	−3.96530	6.27599	−4.29618
−4.66790	6.81830	−3.33902	−5.37935	7.36902	−2.39785	−5.61163	7.54519	−1.12658	−5.86052	7.73724	0.13815

Table A7. Cartesian coordinates of $4C_{26}$ cyclic cumulene conformer 1 having HF 6-311G* optimal geometry.

5.17522	−2.16282	−0.01977	5.56532	−1.03759	−0.07769	5.63702	0.33740	−0.13549	5.37488	1.50006	−0.17104
4.75927	2.73256	−0.19280	4.00232	3.65404	−0.19612	2.92835	4.51716	−0.18631	1.86519	5.05698	−0.16723
0.52738	5.38546	−0.13588	−0.66453	5.37750	−0.10275	−1.98708	4.99293	−0.05690	−2.99345	4.35516	−0.01090
−3.92624	3.34283	0.05024	−4.50001	2.29896	0.10662	−4.89440	0.98032	0.17059	−4.99399	−0.20692	0.22177
−4.81304	−1.57200	0.26983	−4.39339	−2.68781	0.29825	−3.59025	−3.80752	0.31106	−2.65626	−4.54861	0.30416
−1.38440	−5.07842	0.28011	−0.20326	−5.23938	0.24879	1.16844	−5.11679	0.20439	2.30607	−4.76198	0.15996
3.50719	−4.08933	0.10198	4.39863	−3.29912	0.04727	−0.87899	2.63500	−3.09286	−1.34480	3.24110	−4.00690
−2.03747	4.10794	−4.81966	−2.73770	4.95910	−5.27247	−3.61361	6.00017	−5.47461	−4.38687	6.89977	−5.36240
−5.24385	7.87533	−4.90881	−5.91246	8.61673	−4.25841	−6.55384	9.30393	−3.25426	−6.96435	9.71870	−2.21536
−7.24337	9.96135	−0.89054	−7.30220	9.95481	0.29953	−7.15515	9.69771	1.64273	−6.84875	9.27137	2.71237
−6.30909	8.57284	3.76723	−5.70725	7.82364	4.47170	−4.89793	6.84306	4.99647	−4.13837	5.94221	5.17361
−3.24503	4.90402	5.04705	−2.50271	4.05838	4.65514	−1.73136	3.20136	3.90518	−1.17868	2.60589	3.03351
−0.70867	2.12983	1.83195	−0.47517	1.92472	0.68207	−0.40723	1.92980	−0.69105	−0.53058	2.14515	−1.85596
8.07620	0.55943	5.02090	6.88637	0.49654	5.03583	5.55092	0.38891	4.72444	4.49530	0.27160	4.18424
3.46565	0.11470	3.28585	2.79211	−0.02981	2.31359	2.31094	−0.20001	1.03695	2.16715	−0.33865	−0.13691
2.31450	−0.48521	−1.49582	2.71998	−0.58954	−2.61128	3.48911	−0.67819	−3.74810	4.37412	−0.72050	−4.54487
5.58652	−0.72836	−5.19442	6.74039	−0.69851	−5.49025	8.11381	−0.62467	−5.50378	9.26990	−0.53009	−5.23118
10.48786	−0.39250	−4.60702	11.38062	−0.25566	−3.82977	12.16437	−0.08652	−2.71216	12.59041	0.06125	−1.60925
12.76207	0.22321	−0.25419	12.62500	0.34818	0.92282	12.14621	0.46621	2.20685	11.47729	0.54003	3.19017
10.45640	0.58731	4.11076	9.40718	0.59339	4.67549	−0.99910	−1.64745	1.62168	−1.00974	−1.47408	0.25800
−1.16327	−1.55568	−0.91994	−1.50734	−1.91766	−2.20095	−1.93390	−2.45412	−3.17571	−2.54684	−3.29279	−4.07722
−3.14903	−4.16651	−4.61930	−3.88622	−5.28467	−4.93266	−4.52351	−6.29140	−4.91843	−5.21500	−7.42914	−4.57295
−5.74080	−8.33643	−4.00708	−6.22811	−9.23211	−3.08394	−6.52208	−9.83236	−2.09751	−6.69407	−10.28218	−0.80911
−6.68962	−10.43905	0.37207	−6.50774	−10.34085	1.73192	−6.20622	−10.01863	2.83875	−5.71190	−9.39449	3.96035
−5.18172	−8.66630	4.74038	−4.48720	−7.65813	5.36747	−3.84885	−6.69000	5.64151	−3.11292	−5.52801	5.62888
−2.51286	−4.54216	5.33241	−1.90474	−3.49421	4.68135	−1.48166	−2.71856	3.88185	−1.14355	−2.02795	2.74145

Table A8. Cartesian coordinates of $4C_{26}$ cyclic cumulene conformer 2 having HF 6-311G* optimal geometry.

5.01853	−1.97390	−0.05084	5.35855	−0.83697	−0.05211	5.45303	0.55917	−0.05390	5.26859	1.73149	−0.05616
4.73281	3.02418	−0.06039	4.02507	3.97698	−0.06457	2.92685	4.84471	−0.06744	1.83443	5.30885	−0.06808
0.45020	5.51463	−0.06866	−0.73086	5.39831	−0.06932	−2.05693	4.95113	−0.06972	−3.06884	4.33110	−0.06931
−4.06772	3.35078	−0.06992	−4.70397	2.34891	−0.07213	−5.13979	1.01888	−0.07525	−5.20958	−0.16595	−0.07692
−4.93893	−1.53901	−0.07488	−4.43292	−2.61257	−0.07009	−3.55687	−3.70395	−0.06362	−2.62142	−4.43423	−0.05752
−1.34977	−5.01817	−0.05099	−0.18617	−5.25153	−0.04700	1.21122	−5.17964	−0.04494	2.34115	−4.81639	−0.04583
3.51832	−4.05954	−0.04734	4.32586	−3.18984	−0.04936	0.84609	2.30944	−3.14470	0.21994	2.77315	−4.03936
−0.71104	3.44607	−4.83601	−1.61732	4.08859	−5.25234	−2.75412	4.88738	−5.40469	−3.71801	5.55941	−5.24136
−4.78137	6.29994	−4.71734	−5.56898	6.84945	−4.02085	−6.30538	7.37477	−2.95527	−6.73257	7.69342	−1.89547
−6.97399	7.90171	−0.53478	−6.94597	7.92702	0.65083	−6.64198	7.77430	2.00630	−6.16789	7.49485	3.05716
−5.38592	7.00022	4.10469	−4.57149	6.46261	4.77925	−3.49188	5.72437	5.27224	−2.52848	5.04534	5.40693
−1.40845	4.23023	5.22060	−0.52985	3.56681	4.77859	0.35880	2.86261	3.96104	0.94424	2.36783	3.05555
1.41271	1.95422	1.80494	1.60091	1.76741	0.64869	1.58300	1.75814	−0.74965	1.36118	1.92686	−1.90269
7.16651	−0.42237	5.30666	6.02494	−0.71211	5.44880	4.67836	−1.04068	5.27022	3.60479	−1.29209	4.83249
2.49714	−1.53912	4.01673	1.74675	−1.69264	3.11078	1.13210	−1.80736	1.86042	0.86919	−1.84364	0.70422
0.87800	−1.82748	−0.69419	1.15466	−1.76327	−1.84590	1.77907	−1.61312	−3.08751	2.53341	−1.42860	−3.98437
3.64143	−1.14610	−4.78814	4.71261	−0.86720	−5.21488	6.05509	−0.51557	−5.38003	7.19279	−0.21617	−5.22727
8.45028	0.11101	−4.71259	9.38374	0.34906	−4.02021	10.26203	0.56534	−2.95471	10.77759	0.68356	−1.89291
11.08548	0.73681	−0.53069	11.07979	0.70720	0.65514	10.76193	0.58941	2.01098	10.24181	0.42470	3.06431
9.36130	0.16821	4.11897	8.42699	−0.08961	4.80300	−1.88024	0.60188	0.92464	−1.81868	0.61393	−0.47233
−1.87196	0.36479	−1.63080	−2.03659	−0.22329	−2.88805	−2.25401	−0.94357	−3.80519	−2.57481	−2.01218	−4.64687
−2.88611	−3.05519	−5.11849	−3.28146	−4.37623	−5.34586	−3.62241	−5.50842	−5.24988	−4.01402	−6.77184	−4.79845
−4.31902	−7.71787	−4.15077	−4.63206	−8.61334	−3.12412	−4.84307	−9.14451	−2.08453	−5.01474	−9.46707	−0.73535
−5.08627	−9.46884	0.44880	−5.07426	−9.15811	1.81159	−4.98093	−8.64494	2.87708	−4.77249	−7.78232	3.95714
−4.52060	−6.87004	4.67246	−4.15303	−5.64028	5.22601	−3.80012	−4.52445	5.42024	−3.36217	−3.20198	5.30744
−2.99619	−2.14020	4.92523	−2.59542	−1.03816	4.16462	−2.30052	−0.28897	3.29332	−2.03006	0.33051	2.06968

References

1. Gorjizadeh, N.; Farajian, A.A.; Kawazoe, Y. Non-coherent transport in carbon chains. *J. Phys. Condens. Matter.* **2011**, *23*, 75301. [CrossRef] [PubMed]
2. Zhang, Y.; Su, Y.; Wang, L.; Kong, E.S.W.; Chen, X.; Zhang, Y. A one-dimensional extremely covalent material: Monatomic carbon linear chain. *Nanoscale Res. Lett.* **2011**, *6*, 577. [CrossRef]
3. Zirzlmeier, J.; Schrettl, S.; Brauer, J.C.; Contal, E.; Vannay, L.; Brémond, É.; Jahnke, E.; Guldi, D.M.; Corminboeuf, C.; Tykwinski, R.R.; et al. Optical gap and fundamental gap of oligoynes and carbyne. *Nat. Commun.* **2020**, *11*, 4797. [CrossRef] [PubMed]
4. Li, J.-P.; Meng, S.-H.; Lu, H.-T.; Tohyama, T. First-principles study on the mechanics, optical, and phonon properties of carbon chains. *Chin. Phys. B* **2018**, *27*, 117101. [CrossRef]
5. Zhang, K.; Zhang, Y.; Shi, L. A review of linear carbon chains. *Chin. Chem. Lett.* **2020**, *31*, 1746–1756. [CrossRef]
6. Da Silva, C.A.B.; Nisioka, K.R.; Moura-Moreira, M.; Macedo, R.F.; Del Nero, J. Tunneling rules for electronic transport in 1D systems. *Mol. Phys.* **2021**, *119*, e1976427. [CrossRef]
7. Bamdad, M.; Mousavi, H. Harrison model of polyynic carbyne chains. *ECS J. Solid State Sci. Technol.* **2021**, *10*, 031001. [CrossRef]
8. Zheng, P.; Zubatyuk, R.; Wu, W.; Isayev, O.; Dral, P.O. Artificial intelligence-enhanced quantum chemical method with broad applicability. *Nat. Commun.* **2021**, *12*, 7022. [CrossRef] [PubMed]
9. Jäntschi, L. *General Chemistry Course (Version 8)*; AcademicDirect: Cluj-Napoca, Romania, 2017; pp. 36–37.
10. Dubrovinskaia, N.; Dubrovinsky, L. Aggregated diamond nanorods, the densest and least compressible form of carbon. *Appl. Phys. Lett.* **2005**, *87*, 083106. [CrossRef]
11. Itzhaki, L.; Altus, E.; Basch, H.; Hoz, S. Harder than diamond: Determining the cross-sectional area and Young's modulus of molecular rods. *Angew. Chem. Int. Ed.* **2005**, *44*, 7432–7435. [CrossRef]
12. Smith, P.P.K.; Buseck, P.R. Carbyne forms of carbon: Do they exist? *Science* **1982**, *216*, 984–986. [CrossRef] [PubMed]
13. McCarthy, M.C.; Chen, W.; Travers, M.J.; Thaddeus, P. Microwave spectra of 11 polyyne carbon chains. *Astrophys. J.* **2000**, *129*, 611–623. [CrossRef]
14. McCarthy, M.C.; Chen, W.; Travers, M.J.; Thaddeus, P. The strongest and toughest predicted materials: Linear atomic chains without a Peierls instability. *Matter* **2022**, *5*, 1192–1203. [CrossRef]
15. Karpfen, A. Ab initio studies on polymers. I. The linear infinite polyyne. *J. Phys. C: Solid State Phys.* **1979**, *12*, 3227. [CrossRef]
16. Rice, M.J.; Bishop, A.R.; Campbell, D.K. Unusual soliton properties of the infinite polyyne chain. *Phys. Rev. Lett.* **1983**, *51*, 2136–2139. [CrossRef]

17. Rozental, E.; Altus, E.; Major, D.T.; Hoz, S. Shaping polyyne rods by using an electric field. *ChemistryOpen* **2017**, *6*, 733–738. [CrossRef]

18. Jäntschi, L.; Bolboacă, S.D. Conformational study of C_{24} cyclic polyyne clusters. *Int. J. Quantum Chem.* **2018**, *118*, e25614. [CrossRef]

19. Sladkov, A.M.; Kasatochkin, V.I.; Kudryavtsev, Y.P.; Korshak, V.V. Synthesis and properties of valuable polymers of carbon. *Bull. Acad. Sci. USSR Div. Chem. Sci.* **1968**, *17*, 2560–2565. [CrossRef]

20. Brédas, J.L.; Chance, R.R.; Baughman, R.H.; Silbey, R. Ab initio effective Hamiltonian study of the electronic properties of conjugated polymers. *J. Chem. Phys.* **1982**, *76*, 3673–3678. [CrossRef]

21. Akagi, K.; Nishiguchi, M.; Shirakawa, H.; Furukawa, Y.; Harada, I. One-dimensional conjugated carbyne-synthesis and properties. *Synth. Met.* **1987**, *17*, 557–562. [CrossRef]

22. Johnson, B.F.G.; Kakkar, A.K.; Khan, M.S.; Lewis, J. Synthesis of novel rigid rod iron metal containing polyyne polymers. *J. Organomet. Chem.* **1991**, *409*, C12–C14. [CrossRef]

23. Heimann, R.B. Linear finite carbon chains (carbynes): Their role during dynamic transformation of graphite to diamond, and their geometric and electronic structure. *Diam. Relat. Mater.* **1994**, *3*, 1151–1157. [CrossRef]

24. Page, A.J.; Ding, F.; Irle, S.; Morokuma, K. Insights into carbon nanotube and graphene formation mechanisms from molecular simulations: A review. *Rep. Prog. Phys.* **2015**, *78*, 036501. [CrossRef]

25. Anderson, H.L.; Patrick, C.W.; Scriven, L.M.; Woltering, S.L. A short history of cyclocarbons. *Bull. Chem. Soc. Jpn.* **2021**, *94*, 798–811. [CrossRef]

26. Lagow, R.J.; Kampa, J.J.; Han-Chao, W.; Battle, S.L.; Genge, J.W.; Laude, D.A.; Harper, C.J.; Bau, R.; Stevens, R.C.; Haw, J.F.; et al. Synthesis of linear acetylenic Carbon: The "sp" Carbon allotrope. *Science* **1995**, *267*, 362–367. [CrossRef] [PubMed]

27. Eastmond, R.; Johnson, T.R.; Walton, D.R.M. Silylation as a protective method for terminal alkynes in oxidative couplings: A general synthesis of the parent polyynes H(C≡C)$_n$H (n = 4–10. 12). *Tetrahedron* **1972**, *28*, 4601–4616. [CrossRef]

28. Zheng, Q.; Gladysz, J.A. A synthetic breakthrough into an unanticipated stability regime: Readily isolable complexes in which $C_{16} - C_{28}$ polyynediyl chains span two Platinum atoms. *J. Am. Chem. Soc.* **2005**, *127*, 10508–10509. [CrossRef]

29. Gao, E.; Li, R.; Baughman, R.H. Predicted confinement-enhanced stability and extraordinary mechanical properties for Carbon nanotube wrapped chains of linear Carbon. *ACS Nano* **2020**, *14*, 17071–17079. [CrossRef] [PubMed]

30. Anderson, B.D. Cyclic polyynes as examples of the quantum mechanical particle on a ring. *J. Chem. Educ.* **2012**, *89*, 724–727. [CrossRef]

31. Jäntschi, L.; Bolboacă, S.D.; Janežic, D. Cyclic Carbon polyynes. *Carbon Mater. Chem. Phys.* **2016**, *9*, 423–436. [CrossRef]

32. Hoffmann, R. Extended Hückel theory–v: Cumulenes, polyenes, polyacetylenes and C_n. *Tetrahedron* **1966**, *22*, 521–538. [CrossRef]

33. Hutter, J.; Lüthi, H.P.; Diederich, F. Structures and vibrational frequencies of the carbon molecules $C_2 - C_{18}$ calculated by density functional theory. *J. Am. Chem. Soc.* **1994**, *116*, 750–756. [CrossRef]

34. Hunter, J.; Fye, J.; Jarrold, M.F. Annealing C_{60}^+: Synthesis of fullerenes and large Carbon rings. *Science* **1993**, *260*, 784–786. [CrossRef]

35. Springborg, M.; Kavan, L. On the stability of polyyne. *Chem. Phys.* **1992**, *168*, 249–258. [CrossRef]

36. Springborg, M.; Kavan, L. Can linear carbon chains be synthesized? *Synth. Met.* **1993**, *57*, 4405–4410. [CrossRef]

37. Li, P. DFT studies on configurations, stabilities, and IR spectra of neutral carbon clusters. *J. At. Mol. Sci.* **2012**, *3*, 308–322. [CrossRef]

38. Jäntschi, L.; Bálint, D.; Pruteanu, L.L.; Bolboacă, S.D. Elemental factorial study on one-cage pentagonal face nanostructure congeners. *Mater. Discov.* **2016**, *5*, 14–21. [CrossRef]

39. Ehrenfreund, P.; Foing, B.H. Fullerenes and cosmic Carbon. *Science* **2010**, *329*, 1159–1160. [CrossRef] [PubMed]

40. Black, S.P.; Stefankiewicz, A.R.; Smulders, M.M.J.; Sattler, D.; Schalley, C.A.; Nitschke, J.R.; Sanders, J.K.M. Generation of a dynamic system of three-dimensional tetrahedral polycatenanes. *Angew. Chem. Int. Ed.* **2013**, *52*, 5749–5752. [CrossRef]

41. Akita, M.; Tanaka, Y. Carbon-rich organometallics: Application to molecular electronics. *Coord. Chem. Rev.* **2022**, *461*, 214501. [CrossRef]

42. Safarowsky, O.; Windisch, B.; Mohry, A.; Vögtle, F. Nomenclature for catenanes, rotaxanes, molecular knots, and assemblies derived from these structural elements. *J. Prakt. Chem.* **2000**, *342*, 437–444. [CrossRef]

43. Span, R.; Lemmon, E.W.; Jacobsen, R.T.; Wagner, W.; Yokozeki, A. A reference equation of state for the thermodynamic properties of Nitrogen for temperatures from 63.151 to 1000 K and pressures to 2200 MPa. *J. Phys. Chem. Ref. Data* **2000**, *29*, 1361–1433. [CrossRef]

44. Johnson, R.D., III. Experimental data for N2 (Nitrogen diatomic). *NIST Stand. Ref. Database* **2020**, *101*, 1361–1433. Available online: http://cccbdb.nist.gov/exp2x.asp?casno=7727379 (accessed on 12 September 2022).

45. Liu, Z.; Lu, T.; Chen, Q. Comment on "Theoretical investigation on bond and spectrum of cyclo[18]carbon (C_{18}) with sp-hybridized". *J. Mol. Model.* **2021**, *27*, 42. [CrossRef] [PubMed]

46. Hartree, D.R. The wave mechanics of an atom with a non-Coulomb central field. Part I. Theory and methods. *Math. Proc. Cambridge Phil. Soc.* **1928**, *24*, 89–110. [CrossRef]

47. Hartree, D.R. The wave mechanics of an atom with a non-Coulomb central field. Part II. Some results and discussion. *Math. Proc. Cambridge Phil. Soc.* **1928**, *24*, 111–132. [CrossRef]

48. Fock, V.A. Approximation method for solving the quantum mechanical multibody problem. *Z. Phys.* **1930**, *61*, 126–148. (In German) [CrossRef]

49. Fock, V.A. Self-consistent field with substitution for sodium. *Z. Phys.* **1930**, *62*, 795–805. (In German) [CrossRef]

50. Becke, A.D. Density-functional exchange-energy approximation with correct asymptotic behavior. *Phys. Rev. A* **1988**, *38*, 3098–3100. [CrossRef]

51. Perdew, J.P. Density-functional approximation for the correlation energy of the inhomogeneous electron gas. *Phys. Rev. B* **1986**, *33*, 8822–8824. [CrossRef]

52. Schrödinger, E. An undulatory theory of the mechanics of atoms and molecules. *Phys. Rev.* **1926**, *28*, 1049–1070. [CrossRef]

53. Sitkiewicz, S.P.; Zalesny, R.; Ramos-Cordoba, E.; Luis, J.P.; Matito, E. How reliable are modern density functional approximations to simulate vibrational spectroscopies? *J. Phys. Chem. Lett.* **2022**, *13*, 5963–5968. [CrossRef] [PubMed]

54. Cotton, A.F.; Wilkinson, G. The heat of formation of ferrocene. *J. Am. Chem. Soc.* **1952**, *74*, 5764–5766. [CrossRef]

55. Jaffé, H.H. The electronic structure of ferrocene. *J. Chem. Phys.* **1953**, *21*, 156–157. [CrossRef]

56. Sánchez, M.; Sabio, L.; Gálvez, N.; Capdevila, M.; Dominguez-Vera, J.M. Iron chemistry at the service of life. *IUBMB Life* **2017**, *69*, 382–388. [CrossRef] [PubMed]

57. Bystritskaya, E.V.; Pomerantsev, A.L.; Rodionova, O.Y. Nonlinear regression analysis: New approach to traditional implementations. *J. Chemom.* **2000**, *14*, 667–692.

58. Lin, Y.; Connell, J.W. Advances in 2D Boron nitride nanostructures: Nanosheets, nanoribbons, nanomeshes, and hybrids with graphene. *Nanoscale* **2012**, *4*, 6908–6939. [CrossRef] [PubMed]

59. Stock, A.; Pohland, E. Boron hydrogens, VIII. For knowledge of the B_2H_6 and the B_5H_{11}. *Berichte* **1926**, *59*, 2210–2215. (In German) [CrossRef]

60. Mulliken, R.S. The vibrational isotope effect in the brand spectrum of Boron nitride. *Science* **1923**, *58*, 164–166. [CrossRef]

61. Chopra, N.G.; Luyken, R.J.; Cherrey, K.; Cohen, M.L.; Louie, S.G.; Zettl, A. Boron nitride nanotubes. *Science* **1995**, *269*, 966–967. [CrossRef]

62. Kawaguchi, M.; Kuroda, S.; Muramatsu, Y. Electronic structure and intercalation chemistry of graphite-like layered material with a composition of BC_6N. *J. Phys. Chem. Solids* **2008**, *69*, 1171–1178. [CrossRef]

63. Shi, Z.; Yuan, Q.; Wang, Y.; Nishimura, K.; Yang, G.; Zhang, B.; Jiang, N.; Li, H. Optical properties of bulk single-crystal diamonds at 80–1200 K by vibrational spectroscopic methods. *Materials* **2021**, *14*, 7435. [CrossRef] [PubMed]

64. Susniak, K.; Krysa, M.; Kidaj, D.; Szymanska-Chargot, M.; Komaniecka, I.; Zamlynska, K.; Choma, A.; Wielbo, J.; Ilag, L.L.; Sroka-Bartnicka, A. Multimodal spectroscopic imaging of pea root nodules to assess the Nitrogen fixation in the presence of biofertilizer based on nod-factors. *Int. J. Mol. Sci.* **2021**, *22*, 12991. [CrossRef] [PubMed]

65. Alberti, S.; Datta, A.; Jágerská, J. Integrated nanophotonic waveguide-based devices for IR and Raman gas spectroscopy. *Sensors* **2021**, *21*, 7224. [CrossRef]

66. Born, M.; Oppenheimer, J.R. Zur Quantentheorie der Molekeln. *Ann. Phys.* **1927**, *389*, 457–484. [CrossRef]

67. Johnson, B.G.; Gill, P.M.W.; Pople, J.A. The performance of a family of density functional methods. *J. Chem. Phys.* **1993**, *98*, 5612–5626. [CrossRef]

68. Hunt, K.L.C.; Harris, R.A. Vibrational circular dichroism and electric-field shielding tensors: A new physical interpretation based on non local susceptibility densities. *J. Chem. Phys.* **1991**, *94*, 6995–7002. [CrossRef]

69. Pearson, R.G. Symmetry rule for predicting molecular structure and reactivity. *J. Am. Chem. Soc.* **1969**, *91*, 1252–1254. [CrossRef]

70. Ghanty, T.K.; Ghosh, S.K. A density functional approach to hardness, polarizability, and valency of molecules in chemical reactions. *J. Phys. Chem.* **1996**, *100*, 12295–12298. [CrossRef]

71. Frisch, M.J.; Pople, J.A.; Binkley, J.S. Self-consistent molecular orbital methods 25. Supplementary functions for Gaussian basis sets. *J. Chem. Phys.* **1984**, *80*, 3265–3269. [CrossRef]